A Non-Linear Approach to Spacecraft Trajectory Control in the Vicinity of a Libration Point

Richard J. Luquette
NASA Goddard Space Flight Center

Robert M. Sanner
University of Maryland, Dept. of Aerospace Engineering

ABSTRACT

An expanding interest in mission design strategies that exploit libration point regions demands the continued development of enhanced, efficient, control algorithms for station-keeping and formation maintenance. This paper discusses the development of a non-linear, station-keeping, control algorithm for trajectories in the vicinity of a libration point. The control law guarantees exponential convergence, based on a Lyaponov analysis. Controller performance is evaluated using FreeFlyer® and MATLAB® for a spacecraft stationed near the L2 libration point in the Earth-Moon system, tracking a pre-defined reference trajectory. Evaluation metrics are fuel usage and tracking accuracy. Simulation results are compared with a linear-based controller for a spacecraft tracking the same reference trajectory. Although the analysis is framed in the context of station-keeping, the control algorithm is equally applicable to a formation flying problem with an appropriate definition of the reference trajectory.

INTRODUCTION

The restricted-three body problem examines the behavior of an infinitesimal mass in the combined gravitational field of two finite masses rotating in an orbit about their common center of mass. Research on this problem began prior to 1772, the year Lagrange published a set of particular solutions known as the Lagrange or libration points. Libration points, defined within a rotating two body system, represent locations within the rotating frame at which the dynamical forces due to gravity and rotation are neutralized. The equilibrium points are grouped in a set of three collinear points, referred to as L1, L2 and L3; and a set of two triangular points, L4 and L5. With our emerging capability to implement space-based missions, a growing research interest is focused on methods for exploiting the dynamics in the vicinity of these points. In particular, this paper builds on the current research associated with control strategies for station-keeping in the vicinity of a Libration point. Earlier works (refs. 1, 2, 3) have focused on linear control strategies, based on linearized dynamical equations. This requires assumptions about the motion of the two primary masses, i.e. either circular or elliptical motion about their common center of mass. Further, the validity of the control design is confined to some local region about the point of linearization, typically a libration point.

This study examines the design and performance of a control strategy based on the full non-linear dynamics associated with the restricted three-body problem. The performance of the control strategy is evaluated using the example of a halo orbit about the L2 point in the Earth-Moon system. Interestingly, the orbits of the Earth and Moon about their barycenter are non-planar and non-elliptic. The controller design is based on the Euler-Lagrange (Hamiltonian) form of the dynamics. This design technique, presented by Slotine and Li (ref. 4), is also explored by de Queiroz, et.al. (ref.5), for an Earth orbiting spacecraft. However, their results cannot be simply extended to the restricted three-body problem, since the governing dynamics are significantly different.

THEORY

The dynamics (1) and kinematics (2) for most physical systems can be expressed in the Hamiltonian (or Euler-Lagrange) form.

$$\mathbf{H(q)} * \dot{\mathbf{v}} + \mathbf{C(q,v)} * \mathbf{v} + \mathbf{E(q,v)} = \mathbf{u} \tag{1}$$

$$\dot{\mathbf{q}} = \mathbf{J(q)} * \mathbf{v} \tag{2}$$

Where:

$\mathbf{q}$ – Configuration Variables
$\mathbf{v}$ – Velocity Variables
$\mathbf{H(q)} = \mathbf{H(q)}^T > \mathbf{0}, \forall \mathbf{q}, \mathbf{v}$
$\mathbf{C(q,v)}$ is defined such that $\dot{\mathbf{H}}(\mathbf{q}) - \mathbf{2} * \mathbf{C(q,v)}$ is skew symmetric for all $\mathbf{q}, \mathbf{v}$.

Assuming $\dot{\mathbf{q}} = \mathbf{v}$, i.e. $\mathbf{J(q)} = \mathbf{I}$, then equations (1) and (2) are combined as

$$\mathbf{H(q)} * \ddot{\mathbf{q}} + \mathbf{C(q,\dot{q})} * \dot{\mathbf{q}} + \mathbf{E(q,\dot{q})} = \mathbf{u} \tag{3}$$

The goal is to compute $\mathbf{u}(t)$, such that the system tracks a desired trajectory, $\mathbf{q_d}(t)$. Define the tracking error as $\mathbf{e(t)} = \mathbf{q(t)} - \mathbf{q_d(t)}$, an auxiliary error metric $\mathbf{s(t)} = \dot{\mathbf{e}}(\mathbf{t}) + \mathbf{\Lambda} * \mathbf{e(t)}$, with $\mathbf{\Lambda} = \mathbf{\Lambda}^T > \mathbf{0}$, and a reference velocity $\dot{\mathbf{q}}_r(\mathbf{t}) = \dot{\mathbf{q}}_d(\mathbf{t}) - \mathbf{\Lambda} * \mathbf{e(t)}$.

$$\mathbf{s(t)} = \dot{\mathbf{q}}(\mathbf{t}) - \dot{\mathbf{q}}_r(\mathbf{t}) \tag{4}$$

Reference (4) proposes the following control law with $\mathbf{K_d} = \mathbf{K_d} > \mathbf{0}$:

$$\mathbf{u(t)} = \mathbf{H(q)} * \ddot{\mathbf{q}}_r + \mathbf{C(q,\dot{q})} * \dot{\mathbf{q}}_r + \mathbf{E(q,\dot{q})} - \mathbf{K_d} * \mathbf{s(t)} \tag{5}$$

Combining equations (3), (4) and (5) yields:

$$\mathbf{H(q)} * \dot{\mathbf{s}}(\mathbf{t}) + \mathbf{C(q,\dot{q})} * \mathbf{s(t)} + \mathbf{K_d} * \mathbf{s(t)} = \mathbf{0} \tag{6}$$

The above closed-loop dynamics drive the tracking error, $\mathbf{e}(t)$, to zero. Before proceeding with the proof, it is beneficial to recall the following corollary to Barbalat's Lemma (ref. 4).

If a scalar function $V(\mathbf{x},t)$ satisfies the following conditions, then $\dot{V}(\mathbf{x},t) \rightarrow 0$, *as* $t \rightarrow \infty$.

- $V(\mathbf{x},t)$ *is lower bounded*
- $\dot{V}(\mathbf{x},t)$ *is negative semi-definite*
- $\dot{V}(\mathbf{x},t)$ *is uniformly continuous in time*

Note: The third condition is met if $\ddot{V}(x,t)$ *is bounded.*

The proof that $\mathbf{e}(t) \rightarrow 0$, is based on a Lyapunov analysis. Consider the following candidate Lyapunov function, and it's derivative (ref. 4).

$$V(\mathbf{s},t) = \tfrac{1}{2}\mathbf{s(t)} * \mathbf{H(t)} * \mathbf{s(t)} \geq 0 \tag{7}$$

$$\begin{aligned} \dot{V}(\mathbf{s},t) &= \mathbf{s(t)} * \mathbf{H(t)} * \dot{\mathbf{s}}(\mathbf{t}) + \tfrac{1}{2}\mathbf{s(t)} * \dot{\mathbf{H}}(\mathbf{t}) * \mathbf{s(t)} \\ &= \mathbf{s(t)} * [-\mathbf{C(q,\dot{q})} - \mathbf{K_d}] * \mathbf{s(t)} + \tfrac{1}{2}\mathbf{s(t)} * \dot{\mathbf{H}}(\mathbf{t}) * \mathbf{s(t)} \\ &= -\mathbf{s(t)} * \mathbf{K_d} * \mathbf{s(t)} + \tfrac{1}{2}\mathbf{s(t)} * [\dot{\mathbf{H}}(\mathbf{t}) - \mathbf{2} * \mathbf{C(q,\dot{q})}] * \mathbf{s(t)} \\ &= -\mathbf{s(t)} * \mathbf{K_d} * \mathbf{s(t)} \leq 0 \end{aligned} \tag{8}$$

(Recall $[\dot{\mathbf{H}}(\mathbf{t}) - 2 * \mathbf{C}(\mathbf{q}, \dot{\mathbf{q}})]$ is skew symmetric, $\mathbf{K}_d = \mathbf{K}_d^T > \mathbf{0}$)

Since $\mathbf{H(t)}$ is positive definite, $V(s,t)$ is non-negative (lower bounded). From equation (8), $\dot{V}(\mathbf{s},t)$ is negative semi-definite. It is assumed $\mathbf{q(t)}$ and $\mathbf{q_d(t)}$ are at least twice differentiable. Therefore, $\dot{V}(\mathbf{s},t)$ is uniformly continuous in time. Thus, Barbalat's Lemma guarantees, $\dot{V}(\mathbf{s},t) \rightarrow 0$, (and $\mathbf{s}(t) \rightarrow 0$) as $t \rightarrow \infty$. Consider $\mathbf{e(t)}$ as the output of a stable linear system, $\mathbf{s(t)} = \dot{\mathbf{e}}(\mathbf{t}) + \mathbf{\Lambda} * \mathbf{e(t)}$, with $\mathbf{s(t)}$ as the input. It follows that $\mathbf{s}(t) \rightarrow 0$, implies $\mathbf{e}(t) \rightarrow 0$. In fact, the system is globally stable, and the tracking error converges to zero exponentially.

This analysis ignores disturbance forces, $\mathbf{F_d}$. Consequently, the control strategy will not yield perfect tracking under a disturbance. However, an adaptive control strategy guarantees the desired tracking, provided the disturbed dynamics assume the linear form:

$$\mathbf{H(q)} * \ddot{\mathbf{q}} + \mathbf{C(q,\dot{q})} * \dot{\mathbf{q}} + \mathbf{E(q,\dot{q})} = \mathbf{Y(q,\dot{q},q_d,\dot{q}_d)} * \mathbf{a}$$

where $\mathbf{Y(q,\dot{q},q_d,\dot{q}_d)}$ is known, and here, $\mathbf{a}$ is a constant, unknown, vector.
Global stability and convergence of the tracking error to zero are guaranteed by the following control law and adaptive rule. The proof is provided in reference [4].

$$\begin{aligned} &\mathbf{u} = \mathbf{Y(q,\dot{q},q_r,\dot{q})} * \hat{\mathbf{a}} - \mathbf{K_d} * \mathbf{s}, \\ &\dot{\hat{\mathbf{a}}} = -\mathbf{\Gamma} * \mathbf{Y(q,\dot{q},q_r,\dot{q})} * \mathbf{s}, \quad \mathbf{\Gamma} = \mathbf{\Gamma}^T > \mathbf{0} \end{aligned} \tag{9}$$

THE RESTRICTED-THREE BODY PROBLEM

Under the assumptions of the restricted-three body problem, the gravitational influence of two primary masses (rotating about their common, inertially-fixed, center of mass) govern the dynamics of a small mass (spacecraft). The spacecraft (S/C) dynamics (per unit mass) in inertial coordinates are given by:

$$\ddot{\mathbf{R}}_{sc} = -GM_1 * \mathbf{R}_{1s} / \left\|\mathbf{R}_{1s}\right\|_2^3 - GM_2 * \mathbf{R}_{2s} / \left\|\mathbf{R}_{2s}\right\|_2^3 + \mathbf{F}_d \tag{10}$$

where:

GM_i	= Gravitational Parameter of Mass i
$\mathbf{R}_{is}$	= Position of S/C with respect to Mass i
$\mathbf{R}_{sc}$	= Position of S/C
$\mathbf{F}_d$	= Disturbance Force

Although (10) fits the Hamiltonian form, it is not expressed in a convenient coordinate frame for defining our desired trajectory. Recalling the stated goal is to follow a trajectory in the vicinity of a Libration point, it is more convenient to express the dynamics in the rotating coordinate frame defined by the motion of the smaller primary.

$$\hat{\mathbf{i}} = \mathbf{R}_2 / \left\|\mathbf{R}_2\right\|_2, \hat{\mathbf{k}} = (\mathbf{R}_2 \times \mathbf{V}_2) / \left\|(\mathbf{R}_2 \times \mathbf{V}_2)\right\|_2, \hat{\mathbf{j}} = \hat{\mathbf{k}} \times \hat{\mathbf{i}}$$

Hence:

$$\mathbf{R} = \mathbf{A}_{ir} * \mathbf{r} \; ; \; \mathbf{A}_{ir} = [\hat{\mathbf{i}}, \hat{\mathbf{j}}, \hat{\mathbf{k}}] \tag{11}$$

Where $\mathbf{r}$ represents the coordinates in the rotating frame.

Differentiating (11) and combining the result with (10), yields:

$$\mathbf{u} = \mathbf{A}_{ir}^T * \mathbf{U} = \mathbf{H} * \ddot{\mathbf{r}} + \mathbf{C} * \dot{\mathbf{r}} + \mathbf{E(r)} + \mathbf{A}_{ir}^T * \mathbf{F}_d \tag{12}$$

where:

$$\mathbf{H} = \mathbf{I}_3$$

$$\mathbf{C} = 2 * \mathbf{A}_{ir}^{T} * \dot{\mathbf{A}}_{ir} = 2 * \mathbf{A}_{ir}^{T} * \mathbf{A}_{ir} * \boldsymbol{\Omega} = 2 * \boldsymbol{\Omega}$$

$$\mathbf{E}(\mathbf{r}) = \mathbf{A}_{ir}^{T} * (\ddot{\mathbf{A}}_{ir} * \mathbf{r} + GM_1 * \mathbf{R}_{1s} / \|\mathbf{R}_{1s}\|_2^3 + GM_2 * \mathbf{R}_{2s} / \|\mathbf{R}_{2s}\|_2^3)$$

$$\boldsymbol{\Omega} = Skew\{(\mathbf{r} \times \mathbf{v}) / \|\mathbf{r}\|_2\}$$

Note: $[\dot{\mathbf{H}}(\mathbf{t}) - 2 * \mathbf{C}(\mathbf{q}, \dot{\mathbf{q}})] = 2 * \boldsymbol{\Omega}$, which is skew symmetric.

It is important to note that $\mathbf{A_{ir}}$, and it's derivatives, are defined by the motion of the two primary masses. Hence, the behavior of $\mathbf{A_{ir}}$ is generally well known for trajectories within our solar system.

CONTROL LAW DESIGN FOR THE THREE-BODY PROBLEM

The results of the two preceding sections combine to generate the control law. Here $\mathbf{F_d}$ is considered a constant, unknown, force in inertial coordinates. This is reasonable, since the significant perturbations (the gravitational influence of other bodies and solar pressure) will be reasonably constant in inertial space over short periods of time. In fact, $\mathbf{F_d}$ is expressed as a combination of known and unknown components. For example, the gravitational forces due to select bodies are directly computed as known disturbances. The remaining disturbances are estimated with the adaptive rule given in (9).

Combining (5) and (9), let

$$\mathbf{u}(t) = \mathbf{A}_{ir}^{T} * \mathbf{U} = \mathbf{H} * \ddot{\mathbf{r}}_r + \mathbf{C}(t) * \dot{\mathbf{r}}_r + \mathbf{E}(\mathbf{r}) - \mathbf{K}_d * \mathbf{s} + \mathbf{A}_{ir}^{T} * \hat{\mathbf{F}}_d$$
$$\text{with } \dot{\hat{\mathbf{F}}}_d = -\boldsymbol{\Gamma} * \mathbf{A}_{ir} * \mathbf{s}, \ \dot{\mathbf{r}}_r = \dot{\mathbf{r}}_d - \boldsymbol{\Lambda} * (\mathbf{r} - \mathbf{r}_d) \tag{13}$$

Expressed in inertial coordinates, the control is:

$$\mathbf{U}(t) = \mathbf{A}_{ir} * [\ddot{\mathbf{r}}_r + \mathbf{C}(t) * \dot{\mathbf{r}}_r + \mathbf{E}(\mathbf{r}) - \mathbf{K}_d * \mathbf{s}] + \hat{\mathbf{F}}_d \tag{14}$$

As previously shown, this control achieves perfect tracking. Note that with zero tracking error, $\mathbf{r_r} = \mathbf{r_d}$. In this case, equation (14) reduces to

$$\mathbf{U}_d(t) = \mathbf{A}_{ir} * [\ddot{\mathbf{r}}_d + \mathbf{C}(t) * \dot{\mathbf{r}}_d + \mathbf{E}(\mathbf{r}_d)] + \hat{\mathbf{F}}_d \tag{15}$$

So, as the tracking error goes to zero, the control effort converges to the exact value required to maintain the desired trajectory. Hence, under this control strategy (and the stated assumptions), optimal control is achieved by optimal trajectory design.

This development assumes the barycenter of the two masses remains inertially "fixed", and the spacecraft state is known. Additional assumptions regarding the relative motion of the primaries are not required. The dynamics model for traditional linear control designs constrain the primaries to planar circular (or elliptic) motion, and require linearization of the dynamics equation about a point (typically a libration point). Therefore, modeling errors are significantly reduced in the nonlinear design. Also, the linear design is locally optimal. In contrast, the nonlinear design is globally optimal, although constrained to the region governed by the restricted three-body dynamics.

SIMULATION

Implementation of the proposed adaptive control law, equation (13), is simulated using FreeFlyer® interfaced with MATLAB®. FreeFlyer® supplied the dynamics model and propagation tool. MATLAB® provides the computational tools to determine the control effort at each time step. Additionally, MATLAB® serves to capture and analyze the simulation data.

The simulation scenario considers a spacecraft stationed in the vicinity of the L2 point in the Earth-Moon system. This choice allows comparison with the linear control design presented by Hoffman (ref. 1). Also, the motion of the Earth/Moon about their barycenter is dynamically complex. It is eccentric, but non-elliptic and non-planar, and thus provides a challenging environment for any tracking problem. The control is successfully simulated as both a continuous and impulsive thrust. The results are similar, therefore all presented cases are based on a continuous thrust model. The linear control law is based on an LQR design of a classic PD controller. The gain matrices are provided in Reference 1, Table 5-II. Initial conditions are set with zero position and velocity error to limit the time required for the system to reach "steady state".

Five separate cases are studied. For each case the location of L2, and the orientation of the rotating coordinates are considered dynamic, determined by the instantaneous position of the Earth and Moon. The goal for cases 1 through 3, is to track the position of L2. For cases 4 and 5, the desired trajectory is a 3600 km halo orbit about the L2 point. The trajectory, based on Reference 1, Equation 3.20, is shown in Figure 1, as it appears in the rotating coordinate frame. For cases 1 through 4, the nonlinear control gains, $\mathbf{K_d}$ and $\mathbf{\Lambda}$, were chosen to be equivalent to the linear control gains. Case 5 is the same as case 4, except the nonlinear control gains are adjusted for improved tracking performance. Perturbations include the gravitational influence of the Sun and Jupiter, and solar pressure. Additionally, the Earth is modeled as a point mass for the cases without perturbations. Under perturbations, the Earth's gravitational field model includes zonal and tesseral terms up to J5. The simulation period is 100 days, starting on January 1, 2000. The integration step size is 600 seconds.

The distinguishing features of the five cases are summarized below:

Case 1	Track L2	Without Adaptation	No Perturbations	
Case 2	Track L2	With Adaptive Law	No Perturbations	
Case 3	Track L2	With Adaptive Law	With Perturbations	
Case 4	Track Halo Orbit	With Adaptive Law	With Perturbations	
Case 5	Track Halo Orbit	With Adaptive Law	With Perturbations	Modified Gains

Simulation results are exhibited in Figures 2 through 4.

Figure 2	Cases 1 through 4	Position Error
Figure 3	Cases 1 through 4	Control Effort
Figure 4	Case 5	Position Error/Velocity Error/Control Effort

Examination of the data leads to several observations. In general, the nonlinear control provides superior tracking with or without adaptation for all cases. Comparing cases 1 and 2, adaptation significantly improves the tracking performance of the nonlinear control. Case 3 shows improved tracking over cases 1 and 2. Although intuition suggests adding the perturbations would degrade performance, Figure 3 provides the necessary insight into the observed behavior. Case 3 requires less control to maintain the desired trajectory, suggesting the perturbations complement the control. This is true since the perturbations affect the motion of both the spacecraft and the position of L2 (indirectly) in a similar fashion. In this case compensation for the unmodeled perturbations are effectively built into the control law through the definition of the desired trajectory. This simplifies the demand on the adaptive rule, yielding improved tracking performance for both the nonlinear and linear control strategies.

As noted above, cases 4 and 5 explore the performance for a 3600 km halo orbit based on a design presented in reference 1. Although this trajectory is not considered optimal, it does provide a basis for comparing the control designs. For case 4, the nonlinear control still yields better tracking performance, but less significant than cases 1 through 3. As previously noted, the control gains are modified in case 5 to improve performance. Gain adjustments, established through a trial process, are limited to increasing the magnitude of $\mathbf{\Lambda}$, by a factor of 5. The modification increased the controller sensitivity to position error. The modification does not optimize the design, rather it demonstrates the controller can achieve improved position tracking without the constraint of matching the gains of the linear control law. Following control gain adjustment, the position tracking error is dramatically reduced, as expected (Figure 4).

Perfect tracking is not observed in the simulated results as the theory predicts. This is attributed to the limitations in the simulation environment, coupled with the large values of the spacecraft position vectors. The position vectors,

inertially referenced to the barycenter of the Earth-Moon system, are on the order of $4x10^8$ meters. Hence, a 40 meter tracking error equates to an accuracy of 10^{-5} percent. A control law based on relative position of two spacecraft eliminates these numerical problems, providing much tighter position tracking, a requirement for tight formation flying. This presents a topic for further research.

As noted, the simulation environment imposes additional limitations which contribute to the non-zero tracking error. The most significant limitation relates to computing the instantaneous acceleration of the Moon relative to the barycenter, a parameter not available as an output from FreeFlyer®. Therefore, the Moon's acceleration was estimated as $(\Delta V/\Delta t)$ for an interval centered at any given instance in time. This introduces numerical error in the computed control, since the desired trajectory is ultimately referenced to the Moon's position, velocity and acceleration. $\ddot{A}_{ir}$ is estimated in a similar fashion, since sufficient data is not available for direct computation. The combined influence of these and other numerical errors result in the non-zero tracking error observed in Case 1. The improved tracking for Case 2 implies the adaptive control is reacting to the computational errors as if the system is subjected to a disturbance force. Therefore, the adaptive control compensates for both unmodeled disturbances and numerical disturbances.

Finally, in each case the linear and nonlinear designs require similar control effort. This is expected since the major component of the control effort is required to maintain the desired trajectory.

Conclusion

An adaptive non-linear control law can be effectively implemented to perfectly track a pre-defined trajectory within the dynamic environment of the restricted, three body problem. These trajectories include orbits about either of the primary masses. Further, as the tracking error tends to zero, the resultant control will converge to its optimal value required for the desired trajectory. Thus, the control will perform optimally with an optimal trajectory.

This control is applicable to maintenance of a "leader/follower" formation. For this case the control is implemented on a "follower" spacecraft with the desired trajectory referenced to a "leader" spacecraft. However, for formation maintenance a control based on relative states between spacecraft is preferred. As future work, this design will be reformulated to base the control on relative states between spacecraft with superior performance expected, due to reduced sources of computational errors.

Finally, noise sources are not considered in this analysis, although the simulation environment introduces computational noise in the results. Therefore, additional work is required to evaluate the performance and stability of this control law when coupled with an appropriate estimator.

References:

1. Hoffman, D.A., "Station-keeping at the Collinear Equilibrium Points of the Earth-Moon System", Lyndon B. Johnson Space Center, Report: JSC-26189, September 1993.

2. Cielaszyk, D., and Wie, B., "New Approach to Halo Orbit Determination and Control", Journal of Guidance Navagation and Control, Vol. 19, No.2, March-April 1996.

3. Cielaszyk, D., and Wie, B., "Halo Orbit Determination and Control for the Elliptic Restricted Three-Body System", AIAA/AAS Astrodynamics Conference, August 1994, AIAA-94-3729-CP.

4. Slotine, J.E. and Li, W., "Applied Nonlinear Control", Prentice Hall, Inc., New Jersey, 1991

5. de Queiroz, M.S., Kapila, V., and Yan, Q., "Adaptive Nonlinear Control of Multiple Spacecraft Formation Flying", Journal of Guidance, Navigation, and Control, Vol. 23, No. 3, May-June 2000.

Figure 1: Sample Desired Trajectory, 3600 km Halo Orbit about Dynamic L2 (Earth-Moon)

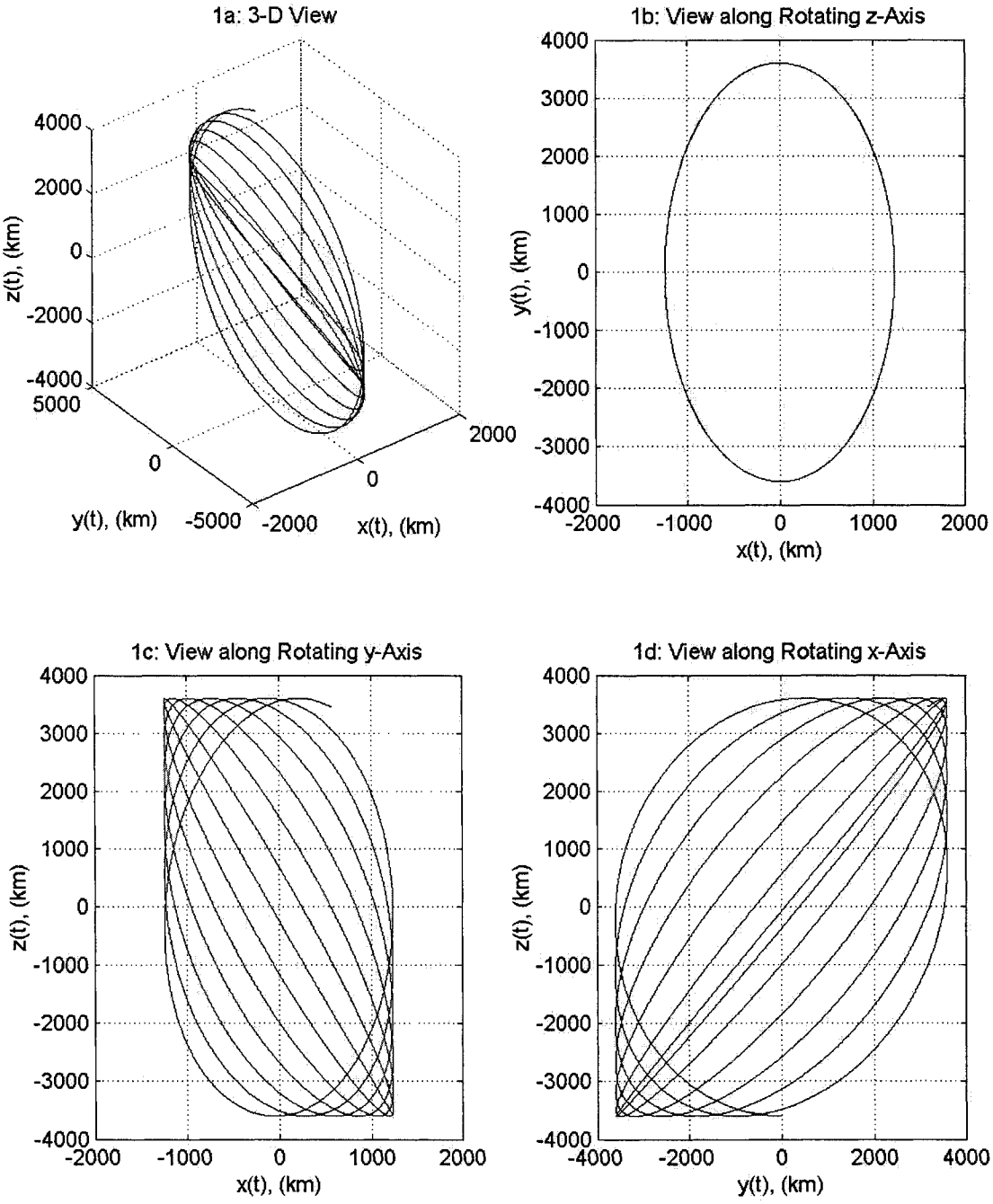

Figure 2: Magnitude of Position Error vs. time

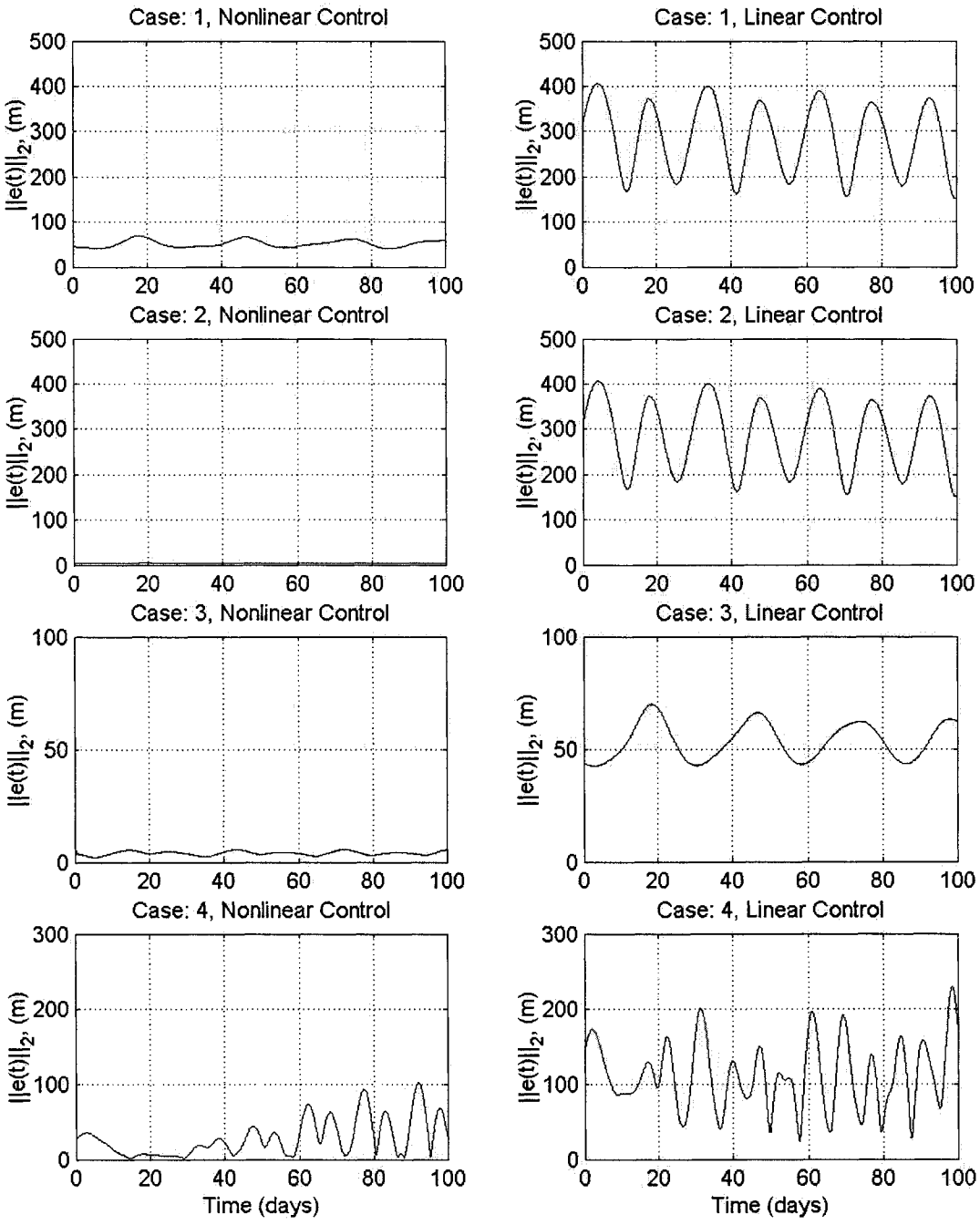

Figure 3: Magnitude of Control Thrust

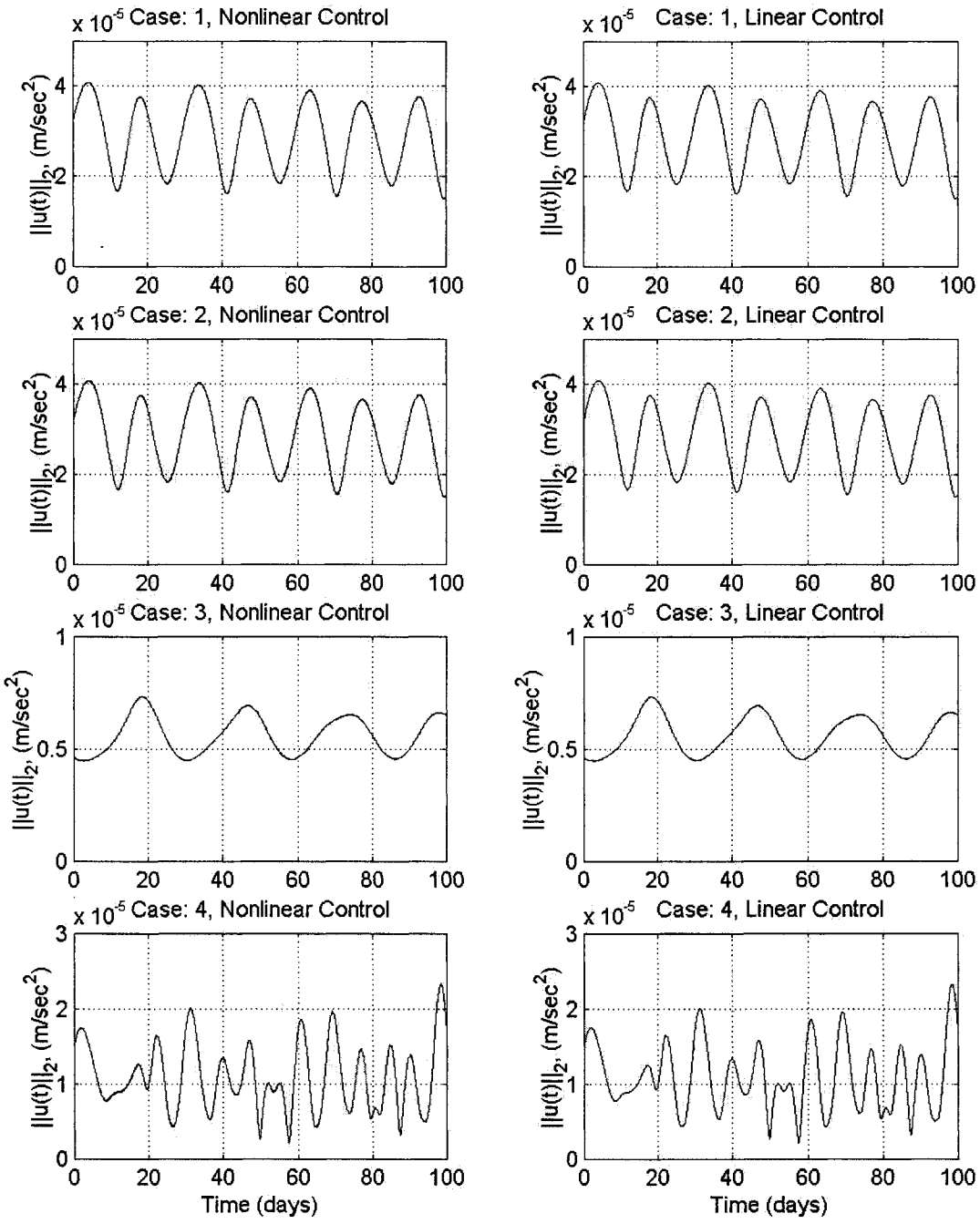

Figure 4: Results for Nonlinear Adaptive Control of a 3600 km Halo Orbit about L2 (Earth-Moon) with Improved Gains